

Received January 9, 2019, accepted January 17, 2019, date of publication January 24, 2019, date of current version February 12, 2019.

Digital Object Identifier 10.1109/ACCESS.2019.2894815

A Study on the Application of Synchronized Chaotic Systems of Different Fractional Orders for Cutting Tool Wear Diagnosis and Identification

HER-TERNG YAU¹, (Senior Member, IEEE), CHENG-CHI WANG², (Member, IEEE),
JIN-YU CHANG¹, AND XIAO-YI SU¹

¹Department of Electrical Engineering, National Chin-Yi University of Technology, Taichung 41170, Taiwan

²Graduate Institute of Precision Manufacturing, National Chin-Yi University of Technology, Taichung 41170, Taiwan

Corresponding author: Her-Terng Yau (pan1012@ms52.hinet.net)

This work was supported in part by the U.S. Department of Commerce under Grant BS123456, and in part by the National Science Council of the Republic of China, Taiwan, under Contract MOST 107-2218-E-167 -001.

ABSTRACT Machining refers to a variety of processes, in which a cutting tool is used to remove the unwanted material from a workpiece. Tool wear, advertently or inadvertently, occurs after long-time use. It is crucial to monitor the tool wear so that the cutting tool can deliver the best performance and meet the technological challenges nowadays. In this paper, through different fractional-order chaotic systems, i.e., Chen–Lee, Lorenz, and Sprott, extension theory is proposed to predict the tool life. The results of the three chaotic systems are compared. The centroid of the 2-D plane of dynamic errors is used as the characteristics. Four wear states are defined in accordance with different levels of surface roughness, i.e., normal, slight, moderate, and severe. The boundaries of the four states are identified according to the locations of the centroid generated with the systems of different fraction orders. The boundaries are then fed into the extension model, and the relational function calculation is performed. In this way, the identification of tool state can be easily achieved. The experiment results indicate that Chen–Lee system and the Lorenz systems exhibit the same diagnosis rate (97.375%), higher than that of the Sprott system (35.75%). It is demonstrated that the two chaotic systems are fit for use with the method proposed in this paper. It is also proven that Chen–Lee and Lorenz fractional-order master–slave chaotic systems are very effective for tool life monitoring. The robustness of diagnosis is also greatly improved.

INDEX TERMS Fractional order chaotic system, cutting, wear, machine tool.

I. INTRODUCTION

As we enter Industry 4.0, various industries, such as electronic component manufacturing, photo-electronics, semiconductors, aerospace technologies, etc., are all moving in the direction of intelligent production in order to catch up the trend of high precision, high yield and small size of products. CNC machine tools play a crucial role in the precision industry. Manufacturing precision, quality, production capacity and tool life of components must all be improved in order to satisfy the high standard required for production. In metal milling process, the cutting is achieved by applying the cutting tool held in the spindle to the workpiece. Although the research papers in the past are mostly focused on the study of spindle [1], [2], cutting tool plays an important role in milling process as well. The quality of products can be greatly improved if the life cycle of cutting tool is

properly controlled. More and more papers about cutting tools have been published [3], [4], meaning that this subject is receiving more and more attention. Bhagat and Nalbalwar [5] use three types of sensors (temperature sensor, accelerometer and current sensor) and Labview software in the experiment. Three tool wear conditions, i.e. initial, normal and severe are defined and data for different parameters are collected. However, the use of many sensors leads to large amount of data and high costs. This method also needs a lot of computing time to determine the characteristic parameters and thus makes it difficult to use in the industry. Niaki *et al.* [6] use wavelet decomposition to extract the statistical characteristics from time and frequency domains. The vibration and power signals are used as input to determine the condition of the cutting tool when used with materials that are difficult to process. Elgargni and Al-Habaibeh [7] also use wavelet

analysis to process infrared images and the power of the spindle and recognize the condition of cutting tool. Therefore, the wavelet analysis is a technique widely used in monitoring the condition of cutting tool. However, this frequency domain based method requires a lot of time to extract characteristics. In addition, the complicated milling environment in realistic world are accompanied with a great variety of variables that may affect the accuracy of recognition. This method is therefore not appropriate to be used in real-time situations. In this paper, a study is performed on the cutting tool of lathe. The goal is to explore how to identify tool wear condition without relying on experience or visual inspection. The method must also improve production efficiency and overcome the drawbacks of the methods previously mentioned. Thanks to the synchronized chaotic system's high-contrast and high-sensitivity property between output and input, we are able to choose the Centroid as characteristics from the ordered but aperiodic trajectory of dynamic errors generated by chaos attractor [8]. Four tool wear conditions (i.e. normal, slight, moderate and severe) and their respective range of states are defined based on the degree of surface roughness of the workpiece. Extension theory is then applied to transform the state boundaries into mathematic model. The extension distance of the matter-element model is then established. The calculation of relational function helps better clarify the relations between the states and improve the accuracy of identifying tool wear conditions.

In Section 2 of this paper, we will introduce how to use three common fractional order chaotic systems so that the change rate of the system will improve. The architecture that combines characteristic extraction and extension theory will be presented as well. The experiment steps, methods of signal acquisition and feeding into the systems are covered in Section 3. The diagnosis rates of the three methods that integrate fractional order chaotic systems and extension theory are also compared. Lastly, the results of this study are concluded in Section 4.

II. INTRODUCTION TO RELATED THEORIES

A. FRACTIONAL ORDER DIFFERENTIAL EQUATIONS

Generally, systems are mostly modeled with the mathematic equations of integral order. However, a wide variety of physical phenomena are better expressed with the fractional order systems based on their physical meaning. Fractional order systems are widely used in fluid mechanics, signal processing and control theories [10]. The definition of a fractional order system [9] is shown in Equations (1) and (2):

$$D_e^{\pm\alpha} e^m \approx \frac{\Gamma(m+1)}{\Gamma(m+1 \mp \alpha)} e^{m \mp \alpha} \quad (1)$$

$$\frac{d^\alpha e(t)}{dt^\alpha} = \lim_{\Delta t \rightarrow 0} \frac{e(t) - \alpha e(t-t_0)}{(t - (t-t_0))^\alpha} \approx \frac{e(t) - \alpha e(t-t_0)}{(\Delta t)^\alpha} \quad (2)$$

In this paper, fractional order systems are used to provide better description of the characteristics than the systems of integer order do. In order to better describe the characteristics, the interval is chosen to be $0 < \alpha < 1$.

B. CHAOS THEORY

Chaos is a phenomenon in nonlinear systems [11]. A dynamic system will be affected by chaos attractor which exhibits an ordered but aperiodic trajectory. The trajectory is highly sensitive and any small change may lead to significantly different behavior.

C. MASTER-SLAVE CHAOTIC SYSTEM

A synchronized chaotic system consists mainly of master system and slave system [12], [13]. Dynamic errors are generated when different signals are fed into the system. The master and slave systems of the chaotic system are defined below in Equation (3):

$$\begin{cases} \dot{X} = Ax + f(x) \\ \dot{Y} = Ay + f(y) + u \end{cases} \quad (3)$$

where $X \in R^n$ and $Y \in R^n$ are state vectors, A system matrix, $f(x)$ and $f(y)$ nonlinear vectors, u nonlinear control input. Since we are focused on the characteristics of dynamic errors that are generated in the master-slave system tracking, we can therefore let control input $u = 0$.

D. CHEN-LEE CHAOTIC SYSTEM

Chen-Lee chaotic system was proposed in 2004 [1], [13], [14]. Its dynamic equation is expressed in Equation (4):

$$\begin{cases} \dot{x} = -yz + ax \\ \dot{y} = xz + by \\ \dot{z} = \left(\frac{1}{3}\right)xy + cz \end{cases} \quad (4)$$

The above equation can be then rewritten in the form of master-slave system matrix. Its dynamic errors are defines as $e = [e_1, e_2, e_3]$, where $e_1 = x_1 - y_1$, $e_2 = x_2 - y_2$ and $e_3 = x_3 - y_3$, as shown in Equation (5):

$$\begin{bmatrix} \dot{e}_1 \\ \dot{e}_2 \\ \dot{e}_3 \end{bmatrix} = \begin{bmatrix} a & 0 & 0 \\ 0 & b & 0 \\ 0 & 0 & c \end{bmatrix} \begin{bmatrix} e_1 \\ e_2 \\ e_3 \end{bmatrix} + \begin{bmatrix} -e_3 e_2 \\ e_1 e_3 \\ \frac{1}{3} e_1 e_2 \end{bmatrix} \quad (5)$$

where α , β and γ are system parameters. Substitute the definition equation of fractional order system (1) into the Chen-Lee system equation(5) as shown in Equations (6) and (7):

$$\frac{d^{-\alpha}}{dt^{-\alpha}} \begin{bmatrix} \dot{e}_1 \\ \dot{e}_2 \\ \dot{e}_3 \end{bmatrix} \approx \begin{bmatrix} \alpha & 0 & 0 \\ 0 & \beta & 0 \\ 0 & 0 & \gamma \end{bmatrix} \frac{d^{+\alpha}}{dt^{+\alpha}} \begin{bmatrix} e_1^1 \\ e_2^1 \\ e_3^1 \end{bmatrix} + \frac{d^{+\alpha}}{dt^{+\alpha}} \begin{bmatrix} -e_3 e_2 e_1^0 \\ e_3 e_1 e_2^0 \\ \frac{1}{3} e_2 e_1 e_3^0 \end{bmatrix} \quad (6)$$

$$\Rightarrow \begin{bmatrix} D^\alpha e_1 \\ D^\alpha e_2 \\ D^\alpha e_3 \end{bmatrix} \approx \begin{bmatrix} a' & 0 & 0 \\ 0 & b' & 0 \\ 0 & 0 & c' \end{bmatrix} \begin{bmatrix} e_1^{1+\alpha} \\ e_2^{1+\alpha} \\ e_3^{1+\alpha} \end{bmatrix} + \begin{bmatrix} -\Gamma(1)e_2 e_3 e_1^\alpha \\ \frac{\Gamma(1+\alpha)}{\Gamma(1+\alpha)} \\ \frac{\Gamma(1)e_1 e_3 e_2^\alpha}{\Gamma(1+\alpha)} \\ \frac{\Gamma(1)e_1 e_2 e_3^\alpha}{3\Gamma(1+\alpha)} \end{bmatrix} \quad (7)$$

where $\rho = (1 - \alpha)$, ρ the fractional order, Γ the gamma function. To realize the behavior of dynamic errors between master and slave systems, we can let $e_1 [i] = x_1 [i] - y_1 [i]$, $e_2 [i] = x_2 [i] - y_2 [i]$ and $e_3 [i] = x_3 [i] - y_3 [i]$. The system equation of the dynamic errors of the synchronized chaotic system is defined in Equation (8). Its parameters are shown in Equation (9):

$$\begin{bmatrix} E1[i] \\ E2[i] \\ E3[i] \end{bmatrix} = \begin{bmatrix} a' & 0 & 0 \\ 0 & b' & 0 \\ 0 & 0 & c' \end{bmatrix} \begin{bmatrix} e_1[i]^{1+\alpha} \\ e_2[i]^{1+\alpha} \\ e_3[i]^{1+\alpha} \end{bmatrix} + \begin{bmatrix} -\Gamma(1)e_2[i]e_3[i](e_1[i])^\alpha \\ \frac{\Gamma(1+\alpha)}{\Gamma(1)e_1[i]e_3[i](e_2[i])^\alpha} \\ \frac{\Gamma(1+\alpha)}{\Gamma(1)e_1[i]e_2[i](e_3[i])^\alpha} \end{bmatrix} \quad (8)$$

$$a' = \frac{a\Gamma(2)}{\Gamma(2+\alpha)}, \quad b' = \frac{b\Gamma(2)}{\Gamma(2+\alpha)}, \quad c' = \frac{c\Gamma(2)}{\Gamma(2+\alpha)} \quad (9)$$

E. LORENZ CHAOTIC SYSTEM

Lorenz chaotic system was proposed in 1963 by Edward Norton Lorenz [15]. Its dynamic equation [16] is shown in Equation (10):

$$\begin{cases} \dot{x} = b(y - x) \\ \dot{y} = bx - y - xz \\ \dot{z} = xy + cz \end{cases} \quad (10)$$

The above equation can be then rewritten in the form of master-slave system matrix. Its dynamic errors are defined as $e = [e_1, e_2, e_3]$, where $e_1 = x_1 - y_1$, $e_2 = x_2 - y_2$ and $e_3 = x_3 - y_3$, as shown in Equation (11).

$$\begin{bmatrix} \dot{e}_1 \\ \dot{e}_2 \\ \dot{e}_3 \end{bmatrix} = \begin{bmatrix} -a & a & 0 \\ b & -1 & 0 \\ 0 & 0 & -c \end{bmatrix} \begin{bmatrix} e_1 \\ e_2 \\ e_3 \end{bmatrix} + \begin{bmatrix} 0 \\ -e_1e_3 \\ e_1e_2 \end{bmatrix} \quad (11)$$

Substitute the definition equation of fractional order system (1) into the Lorenz system equation (11) as shown in Equations (12) and (13).

$$\begin{bmatrix} E1[i] \\ E2[i] \\ E3[i] \end{bmatrix} = \begin{bmatrix} -a' & a' & 0 \\ b' & 0 & 0 \\ 0 & 0 & -c' \end{bmatrix} \begin{bmatrix} e_1[i]^{1+\alpha} \\ e_2[i]^{1+\alpha} \\ e_3[i]^{1+\alpha} \end{bmatrix} + \begin{bmatrix} \frac{-\Gamma(1)(e_1[i])^\alpha}{\Gamma(1+\alpha)} \\ \frac{\Gamma(1)e_1[i]e_3[i](e_2[i])^\alpha}{\Gamma(1+\alpha)} \\ \frac{\Gamma(1)e_1[i]e_2[i](e_3[i])^\alpha}{\Gamma(1+\alpha)} \end{bmatrix} \quad (12)$$

$$a' = \frac{\alpha\Gamma(2)}{\Gamma(2+\alpha)}, \quad b' = \frac{\beta\Gamma(2)}{\Gamma(2+\alpha)}, \quad \gamma' = \frac{\gamma\Gamma(2)}{\Gamma(2+\alpha)} \quad (13)$$

F. SPROTT CHAOTIC SYSTEM

Sprott system is a common chaotic system. Its dynamic equation [15] is shown in Equation (14):

$$\begin{cases} \dot{x} = y \\ \dot{y} = z \\ \dot{z} = -az - by - 1.2x + 2sign(x) \end{cases} \quad (14)$$

The above equation can be then rewritten in the form of master-slave system matrix. Its dynamic errors are defined as $e = [e_1, e_2, e_3]$, where $e_1 = x_1 - y_1$, $e_2 = x_2 - y_2$ and $e_3 = x_3 - y_3$, as shown in Equation (15).

$$\begin{bmatrix} \dot{e}_1 \\ \dot{e}_2 \\ \dot{e}_3 \end{bmatrix} = \begin{bmatrix} 0 & 1 & 0 \\ 0 & 0 & 1 \\ -1.2 & -b & -a \end{bmatrix} \begin{bmatrix} e_1 \\ e_2 \\ e_3 \end{bmatrix} + 2 \begin{bmatrix} 0 \\ 0 \\ sign(x) - sign(y) \end{bmatrix} \quad (15)$$

According to the literature, we can let $sign(x_{1m}) - sign(y_{1s}) = 0$ and ignore \dot{e}_1 . The above can then be expressed as a second order system as shown in Equation (16):

$$\begin{bmatrix} \dot{e}_2 \\ \dot{e}_3 \end{bmatrix} = \begin{bmatrix} 0 & 1 \\ -b & -a \end{bmatrix} \begin{bmatrix} e_2 \\ e_3 \end{bmatrix} \quad (16)$$

Substitute the definition equation of fractional order system (2) into the Sprott system equation (16) as shown in Equations (17) and (18).

$$\begin{bmatrix} D_t^\rho e_2 \\ D_t^\rho e_3 \end{bmatrix} \approx \begin{bmatrix} 0 & t' \\ -b & -a \end{bmatrix} \begin{bmatrix} e_2(t) \\ e_3(t) \end{bmatrix} + \begin{bmatrix} 0 & -kt' \\ -kb' & -ka' \end{bmatrix} \begin{bmatrix} e_2(t - t_0) \\ e_3(t - t_0) \end{bmatrix} \quad (17)$$

$$a' = \frac{a}{\Delta t^\alpha}, \quad Bb' = \frac{b}{\Delta t^\alpha}, \quad Bt' = \frac{1}{\Delta t^\alpha} \quad (18)$$

In this paper, the signals of a brand new cutting tool and the signals collected by sensors are fed to the master and slave systems, respectively. The dynamic errors generated and Centroid are located. The use of fractional order systems makes the change of the systems and characteristics more obvious so that the trend analysis of tool life can be made easy.

G. EXTENSION THEORY

Extension theory was first proposed by Chinese scholar Cai Wen in 1983 to solve fuzzy problems in things. The theory explores the rules among the states using the extension property of matters, which are transformed into mathematic form in order to facilitate categorization [17]. Extension theory consists of two parts, matter-element model and extension set. In classical mathematics, only 0 and 1 are used to represent the property of things. However, there exists a fuzzy area over (0, 1). Fuzzy theory is therefore developed to solve the problem in this interval. Extension theory, which is based on fuzzy theory, extends the relation of things to -1 and 1 after normalization; the negative domain is represented within the red box in Figure 1 below, which extends things to $(-\infty, \infty)$ based on the extension theory and its negative domain (x-axis) can be extended to $-\infty$ and ∞ . Figure 1(a) shows the extent of property that things have or do not have.

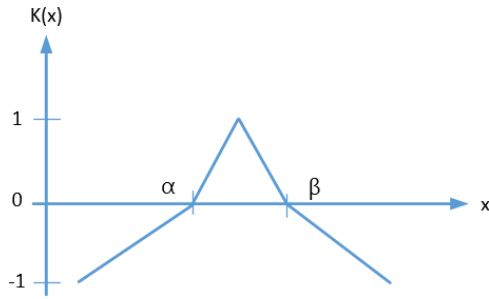


FIGURE 1. Schematic diagram of extension set.

To apply extension theory, the definition of things and state phenomena must be given and added into the matter-element model as shown in Equation (19):

$$R = \begin{bmatrix} N & C_1 & v_1 \\ & C_2 & v_2 \\ & \vdots & \vdots \\ & C_i & v_i \end{bmatrix} \quad (19)$$

where N is the name of the matter, C the characteristic of the matter, v the value of C and i the number of the values. Based on the distance or range of the state phenomena defined, the classical field $V_o = (a, b)$ and segment field $V_p = (a, b)$ are defined as well. The extension distance τ is then defined in Equation (20):

$$\tau(v_i, V_{oi}) = \left| x - \frac{a_{oi} - b_{oi}}{2} \right| - \frac{b_{oi} - a_{oi}}{2}$$

$$\tau(v_i, V_{pi}) = \left| x - \frac{a_{pi} - b_{pi}}{2} \right| - \frac{b_{pi} - a_{pi}}{2}$$

$$i = 1, 2, 3, \dots, n \quad (20)$$

Once the classical field and segment field are defined, the relational function can be calculated as in Equation (21):

$$K_i(v_i) = \begin{cases} \frac{-\tau(v_i, V_{oi})}{|V_{oi}|}, & v_i \in V_{oi} \ \& \ \tau(v_i, V_{pi}) = \tau(v_i, V_{oi}) \\ \frac{\tau(v_i, V_{pi})}{\tau(v_i, V_{pi}) - \tau(v_i, V_{oi})}, & v_i \notin V_{oi} \end{cases} \quad (21)$$

In this paper, the current tool wear condition can be identified by selecting appropriate fractional order, feeding the boundary of Centroid of cutting tool state into the matter-element model and constructing/calculating the relational function. Figure 2 shows the system's architecture and flowchart.

III. EXPERIMENT STEPS AND RESULTS

The above figure shows the system architecture of this paper. This paper captures the vibration signals of lathe turning and substitutes the captured vibration signals into the master-slave chaotic system. The master system represents the turning vibration signals when the tool is in healthy state, while the slave system represents the actual captured signals

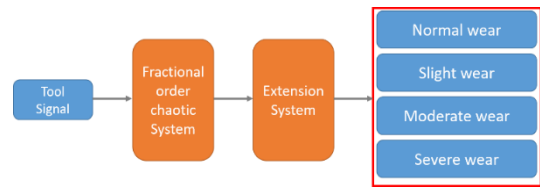


FIGURE 2. System architecture/flowchart diagram.

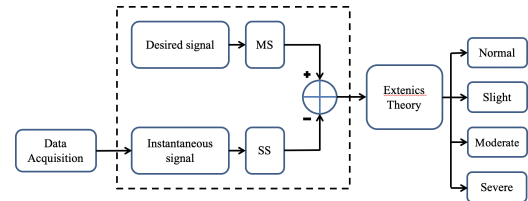


FIGURE 3. System architecture.

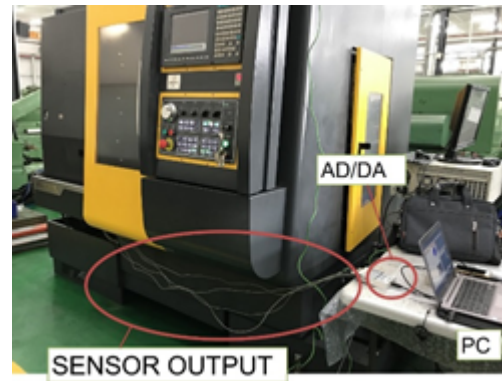


FIGURE 4. The milling setup for measurement and experiment.

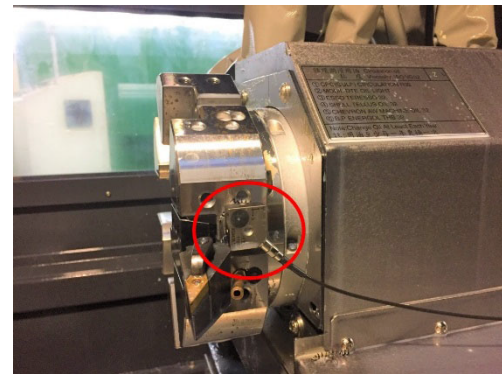


FIGURE 5. The position of accelerometer.

during the manufacturing process. The master-slave chaotic system is defined in Equation (3). The chaotic dynamic errors are generated by the output differences between the master and slave systems, and the chaotic attractor extracted from the dynamic error is then substituted into the extension system, for the subsequent malfunction diagnosis in this paper. The aim of this paper is to perform precision turning on 30*175 (mm*mm) cylinders with machine tool.



FIGURE 6. Four tool wear levels based on the degree of roughness on workpiece surface.

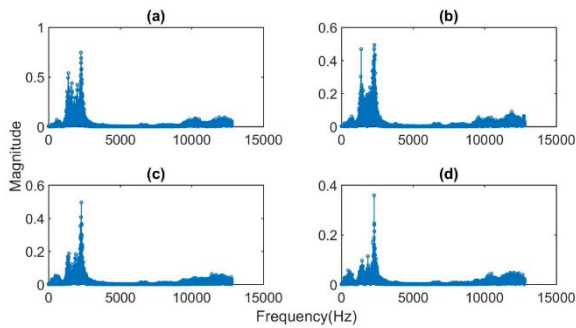


FIGURE 7. Frequency-domain plots for four tool wear levels.

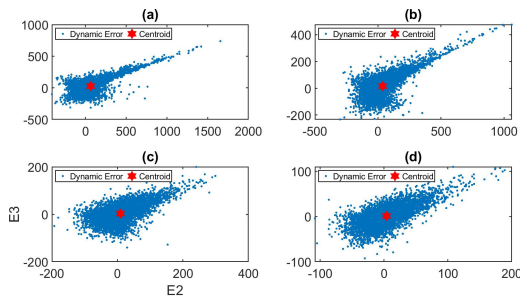


FIGURE 8. Schematic diagram of dynamic errors of cutting tool and its Centroid.

After carrying through and repeating the processing process several times, we carry out an analysis for the vibration signals of turning processing through three different master-slave chaotic systems, and we also utilize extension theory as a subsequent diagnostic tool. Figure 4 shows the hybrid sphere CNC lathe MC4200BL (manufactured by MIKE Machine Industry Co., LTD.) used in the long-time linear milling experiment.

Figure 5 shows the KS943B.100 accelerometers (manufactured by Metra Mess-und Frequenztechnik), which is attached to the turret with magnet. The acceleration signals are picked and measured with National Instruments NI-9234 signal acquisition module and NI USB 9162 module carrier. The surface roughness of each workpiece milled is recorded

TABLE 1. Milling parameters.

Cutting tool name	Mitsubishi tungsten carbide turning insert
Workpiece size (mm*mm)	S45C Ø30*175
Spindle speed (rpm)	1500
Feed rate (mm/rev)	0.2
Cutting thickness (mm)	1
Sampling rate (Hz)	25.6k

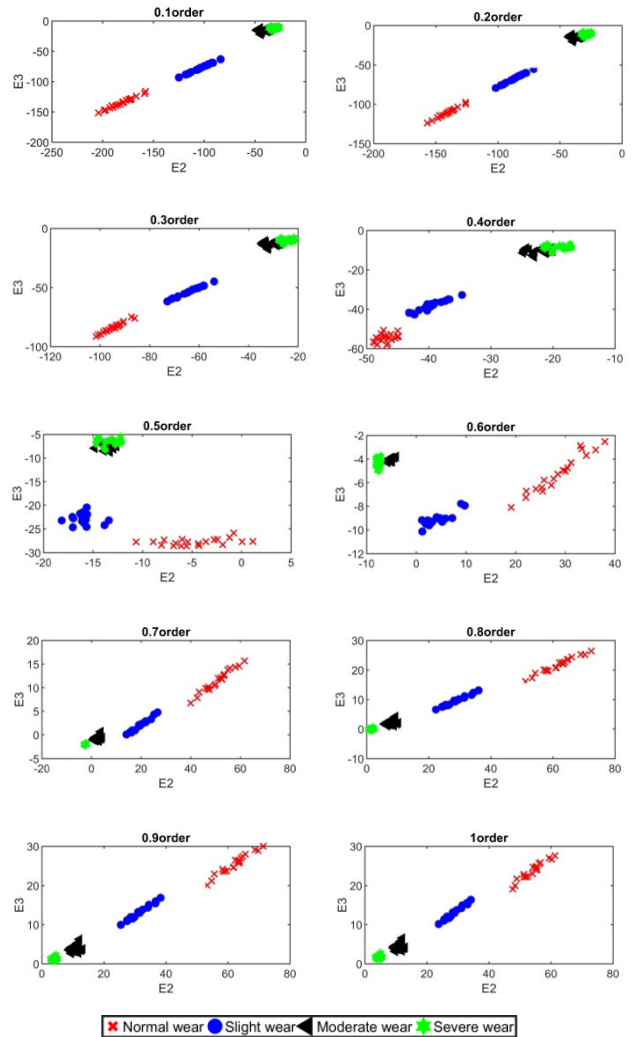


FIGURE 9. Distribution diagram of Centroid of tool wear for Chen-Lee chaotic systems of different fractional orders.

using magnifier. The machining conditions and extracted parameters are shown in Table 1.

Based on the degree of roughness on workpiece surface, four tool wear levels (i.e. normal, slight, moderate and severe) are defined and shown in Figure 6, and according to the ISO standard and the tool wear definition of Kurada and Bradley [17] a corresponding precision comparison table of cutting products is as shown in Table 2. The corresponding signals are stored in the database for this experiment. 40 sets of data are collected for each tool wear

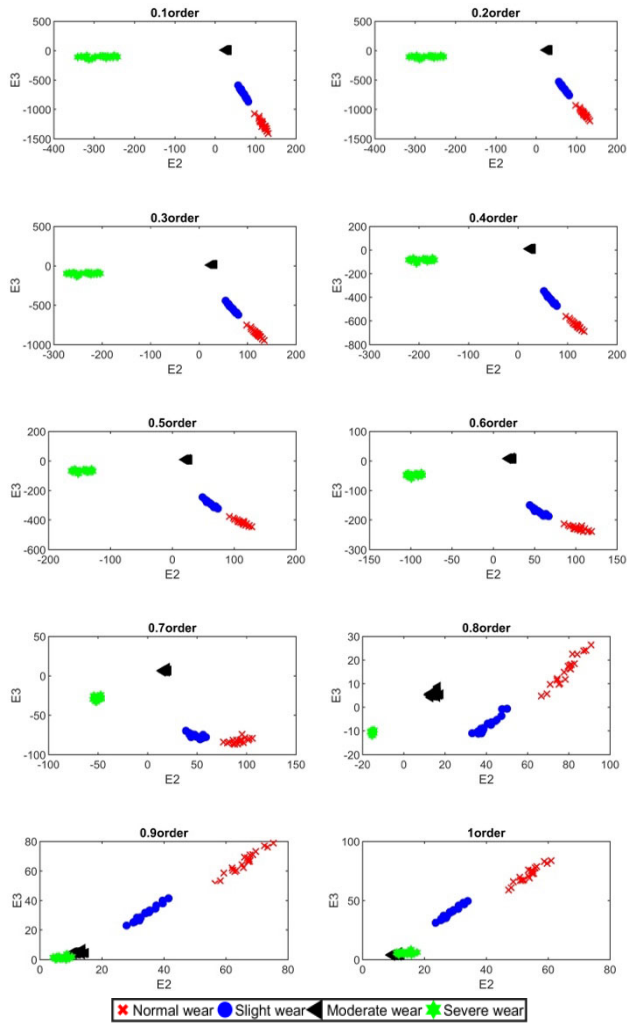


FIGURE 10. Distribution diagram of Centroid of tool wear for Lorenz chaotic systems of different fractional orders.

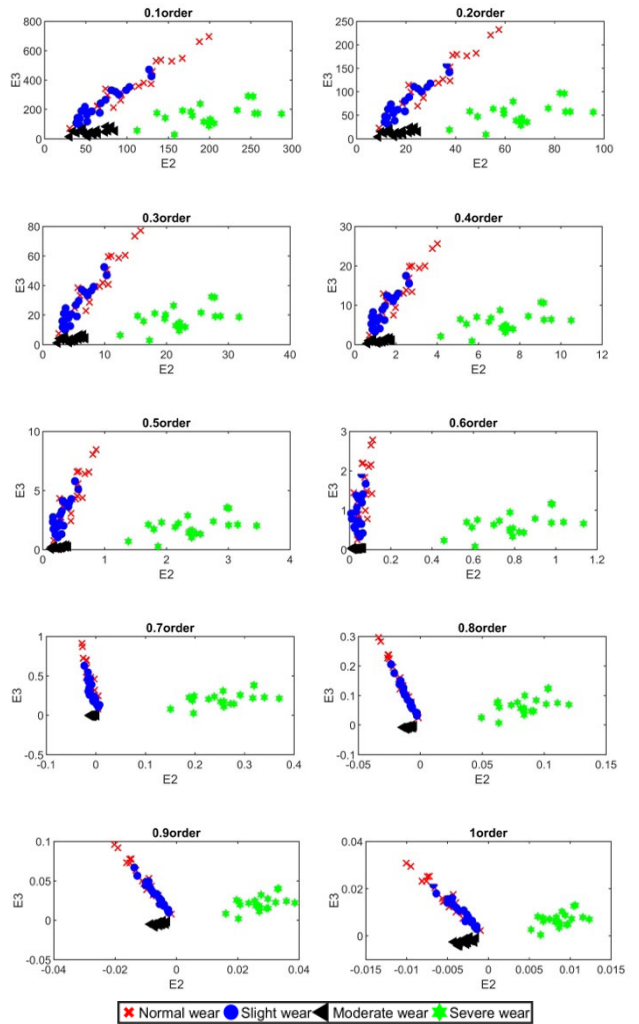


FIGURE 11. Distribution diagram of Centroid of tool wear for Sprott chaotic systems of different fractional orders.

TABLE 2. Tool wear levelsState.

State	Area of tool wear (mm)
Normal	<0.2
Slight	>0.2
Moderate	>0.4
Severe	>0.6

level, with 20 sets to be used to build the model and the other 20 sets to be used for system verification.

MATLAB software is used in the experiment of this study. The signals from machining process are used to build and verify the systems. The different results of three fractional order chaotic systems combined with extension theory are compared. Their diagnosis rates are calculated as well. Figure 7 shows the frequency-domain plots of the signals of four tool wear levels.

The frequency-domain plots of the four tool wear levels, i.e normal, slight, moderate and severe, are shown in Figures 7(a)~(d), respectively. It can be seen that no obvious characteristics in frequency domain can be used as references

for wear level change. As described previous in Section 1, it is a time-consuming task to select characteristics by using traditional methods. In this study, the data are fed into the system and chaotic dynamic errors are generated. The characteristic points are extracted as shown in Figure 8.

Figures 8(a)~(d) show the chaotic dynamic trajectories of the four tool wear levels, i.e. normal, slight, moderate and severe, respectively. It can be seen that the distribution of dynamic errors changes accordingly with tool wear condition. The position of Centroid changes too. The use of fractional order system makes the position change of Centroid more obvious. In this paper, the data are fed into three different fraction order chaotic systems. The plots of Centroid distribution for tool wear condition at orders 0.1~1 are shown in Figures 9 to 11.

The diagrams in Figures 9 to 11 are plotted with the first 20 sets of data of the four tool wear conditions. It can be seen that the Chen-Lee system exhibits an ambiguous distribution of Centroid for moderate and severe wear levels between

Chen-Lee System		Loranz System	
0.1 order	0.2 order	0.1 order	0.2 order
<i>Normal wear</i> E2 [-204.0146, -157.8028] E3 [-151.6579, -116.4668]	<i>Normal wear</i> E2 [-156.7635, -125.8098] E3 [-124.0289, -97.8257]	<i>Normal wear</i> E2 [97.10682, 131.0153] E3 [-1409.82, -1077.02]	<i>Normal wear</i> E2 [97.67354, 132.6191] E3 [-1196.84, -931.735]
<i>Slight wear</i> E2 [-124.8309, -83.8347] E3 [-93.2345, -63.1208]	<i>Slight wear</i> E2 [-101.7194, -71.0936] E3 [-79.4553, -55.4282]	<i>Slight wear</i> E2 [56.6154, 81.77899] E3 [-868.577, -590.251]	<i>Slight wear</i> E2 [56.01457, 81.58654] E3 [-760.819, -529.016]
<i>Moderate wear</i> E2 [-49.9584, -34.5063] E3 [-36.3103, -25.9776]	<i>Moderate wear</i> E2 [-42.6415, -31.6212] E3 [-33.0638, -24.2899]	<i>Moderate wear</i> E2 [22.79507, 33.43143] E3 [-340.824, -242.221]	<i>Moderate wear</i> E2 [22.87089, 33.05825] E3 [-314.883, -229.334]
<i>Sever wear</i> E2 [-21.9885, -11.6421] E3 [-16.3826, -8.7205]	<i>Sever wear</i> E2 [-33.0638, -24.2899] E3 [-15.6105, -8.6829]	<i>Sever wear</i> E2 [7.723232, 4.20479] E3 [-152.33, -81.3455]	<i>Sever wear</i> E2 [8.003495, 14.59539] E3 [-146.927, -81.5162]
0.3 order	0.4 order	0.3 order	0.4 order
<i>Normal wear</i> E2 [-101.551, -85.9529] E3 [-91.4567, -74.9404]	<i>Normal wear</i> E2 [-48.9226, -44.8608] E3 [-58.1553, -50.7089]	<i>Normal wear</i> E2 [98.0091, 134.5273] E3 [-947.2, -753.414]	<i>Normal wear</i> E2 [96.52618, 133.7044] E3 [-688.81, -562.154]
<i>Slight wear</i> E2 [-72.8022, -53.9039] E3 [-61.9117, -44.8939]	<i>Slight wear</i> E2 [-43.1728, -34.6449] E3 [-42.8082, -32.8006]	<i>Slight wear</i> E2 [54.78049, 80.84142] E3 [-623.642, -444.745]	<i>Slight wear</i> E2 [52.46202, 78.42617] E3 [-472.466, -346.802]
<i>Moderate wear</i> E2 [-34.4962, -26.5964] E3 [-27.9634, -21.1558]	<i>Moderate wear</i> E2 [-24.8199, -20.0158] E3 [-21.5913, -16.9363]	<i>Moderate wear</i> E2 [22.33615, 32.04131] E3 [-273.492, -204.255]	<i>Moderate wear</i> E2 [21.10212, 30.26323] E3 [-221.049, -169.366]
<i>Sever wear</i> E2 [-17.5823, -10.4936] E3 [-13.8727, -8.1099]	<i>Sever wear</i> E2 [-13.5059, -8.7919] E3 [-11.3349, -7.0263]	<i>Sever wear</i> E2 [7.99137, 14.59769] E3 [-133.352, -77.0014]	<i>Sever wear</i> E2 [7.661187, 14.13929] E3 [-112.803, -67.9572]
0.5 order	0.6 order	0.5 order	0.6 order
<i>Normal wear</i> E2 [-10.6539, 1.1417] E3 [-28.6295, -25.8649]	<i>Normal wear</i> E2 [19.1175, 37.9575] E3 [-8.1099, -2.5378]	<i>Normal wear</i> E2 [92.4264, 128.6226] E3 [-446.284, -376.913]	<i>Normal wear</i> E2 [85.65819, 119.1076] E3 [-239.392, -213.685]
<i>Slight wear</i> E2 [-18.1639, -13.4058] E3 [-24.6652, -20.4809]	<i>Slight wear</i> E2 [1.1295, 9.7314] E3 [-10.1397, -7.7776]	<i>Slight wear</i> E2 [48.90136, 73.83905] E3 [-322.568, -245.346]	<i>Slight wear</i> E2 [44.23015, 67.16524] E3 [-187.509, -150.228]
<i>Moderate wear</i> E2 [-14.8412, -12.511] E3 [-14.6928, -12.0854]	<i>Moderate wear</i> E2 [-5.8187, -4.0895] E3 [-8.1587, -7.1333]	<i>Moderate wear</i> E2 [19.2058, 27.74117] E3 [-136.046, -128.422]	<i>Moderate wear</i> E2 [16.9096, 24.63015] E3 [-105.477, -86.0114]
<i>Sever wear</i> E2 [-8.74, -6.5071] E3 [-8.2602, -5.5238]	<i>Sever wear</i> E2 [-4.2897, -3.7856] E3 [-4.9862, -3.7595]	<i>Sever wear</i> E2 [7.02745, 13.21399] E3 [-87.346, -55.1284]	<i>Sever wear</i> E2 [6.151959, 11.89266] E3 [-59.7407, -39.8546]
0.7 order	0.8 order	0.7 order	0.8 order
<i>Normal wear</i> E2 [39.9694, 61.6967] E3 [6.7553, 15.643]	<i>Normal wear</i> E2 [51.1997, 72.334] E3 [16.155, 26.3644]	<i>Normal wear</i> E2 [76.76929, 106.0199] E3 [-86.954, -74.3874]	<i>Normal wear</i> E2 [66.69276, 90.85104] E3 [4.791774, 26.30594]
<i>Slight wear</i> E2 [14.0965, 26.6216] E3 [0.0859, 4.7398]	<i>Slight wear</i> E2 [22.3205, 36.0762] E3 [6.578, 13.0723]	<i>Slight wear</i> E2 [38.82026, 58.96188] E3 [-80.6563, -69.9779]	<i>Slight wear</i> E2 [33.20054, 50.0813] E3 [-11.1655, -0.64716]
<i>Moderate wear</i> E2 [0.7646, 4.2485] E3 [-2.9629, -1.9374]	<i>Moderate wear</i> E2 [10.1514, 22.3205] E3 [0.606, 2.5354]	<i>Moderate wear</i> E2 [14.45516, 21.20441] E3 [-54.9467, -46.8071]	<i>Moderate wear</i> E2 [12.13402, 17.81927] E3 [-16.1666, -14.3285]
<i>Sever wear</i> E2 [-1.2707, 0.657] E3 [-2.1372, -1.8466]	<i>Sever wear</i> E2 [1.0686, 4.1621] E3 [-0.3709, 0.6395]	<i>Sever wear</i> E2 [5.145509, 10.3229] E3 [-33.1908, -24.0008]	<i>Sever wear</i> E2 [4.162789, 8.716487] E3 [-12.0266, -9.70864]
0.9 order	1 order	0.9 order	1 order
<i>Normal wear</i> E2 [53.2996, 71.3695] E3 [20.0674, 29.991]	<i>Normal wear</i> E2 [47.6768, 61.3104] E3 [19.0496, 27.5744]	<i>Normal wear</i> E2 [56.50968, 75.3104] E3 [51.53636, 78.72262]	<i>Normal wear</i> E2 [47.22903, 60.96789] E3 [58.8625, 83.67588]
<i>Slight wear</i> E2 [25.4682, 38.2846] E3 [9.9261, 6.8417]	<i>Slight wear</i> E2 [23.7871, 34.1979] E3 [10.1174, 6.3433]	<i>Slight wear</i> E2 [27.95487, 41.48129] E3 [22.97871, 41.47491]	<i>Slight wear</i> E2 [23.61862, 34.03136] E3 [31.09875, 49.5698]
<i>Moderate wear</i> E2 [8.7926, 13.1053] E3 [2.8285, 1.397]	<i>Moderate wear</i> E2 [9.315, 12.9365] E3 [3.4296, 5.6663]	<i>Moderate wear</i> E2 [10.25133, 14.85911] E3 [4.319526, 10.33059]	<i>Moderate wear</i> E2 [9.083836, 12.67884] E3 [10.96462, 17.64041]
<i>Sever wear</i> E2 [2.6512, 6.225] E3 [0.7903, 2.2666]	<i>Sever wear</i> E2 [3.169, 6.5206] E3 [1.1968, 2.7262]	<i>Sever wear</i> E2 [3.389747, 7.324965] E3 [0.058336, 3.722808]	<i>Sever wear</i> E2 [3.0238, 6.406183] E3 [3.992535, 8.568212]

FIGURE 12. The matter-element models of tool wear for Chen-Lee chaotic systems of different fractional orders.

orders 0.1 and 0.5. However, the distributions of Centroid at orders 0.6 to 1 become obvious. For Lorenz system, the distributions are obvious with orders 0.1 to 0.8 but begin to exhibit ambiguity with orders 0.9 and 1 for moderate and severe wear levels. The results of Sprott system show that the distribution of Centroid of various orders for severe wear level is more obvious than those for the other three levels. The distributions of Centroid for normal and slight wear levels are overlapping to a great extent. The extension distances of extension models are created based on the results described above and shown in Figures 12 to 14.

The last 20 sets of data are fed into the matter-element models just established. The state is then determined based on

the results of the relational function calculation. The statistics of diagnosis rates are shown in Table 3.

The above table shows that Chen-Lee and Lorenz systems deliver better overall performance. Chen-Lee system even produces 100% diagnosis rate at orders 0.1, 0.4, 0.5, 0.6, 0.8 and 0.9. Lorenz system achieves 100% diagnosis rate at orders 0.2, 0.3, 0.6, 0.7, 0.9 and 1. However, the overall performance delivered by Sprott system is poor. Its diagnosis rate is low due to the ambiguous distribution of Centroid described previously.

FIGURE 13. The matter-element models of tool wear for Lorenz chaotic systems of different fractional orders.

Sprott System

<p>0.1 order</p> <p>[Normal wear E2 [30.53678,199.3205] E3 [69.68689,695.1629]]</p> <p>[Slight wear E2 [38.52477,129.6769] E3 [94.0209,470.8886]]</p> <p>[Moderate wear E2 [30.40332,85.68667] E3 [112.1467,287.3041]]</p> <p>[Sever wear E2 [14.58742,83.39988] E3 [27.7815,290.4953]]</p> <p>0.3 order</p> <p>[Normal wear E2 [2.614817,15.82218] E3 [7.456744,77.14596]]</p> <p>[Slight wear E2 [3.177618,10.34297] E3 [9.982877,52.50567]]</p> <p>[Moderate wear E2 [2.422913,6.932687] E3 [12.53261,31.75604]]</p> <p>[Sever wear E2 [1.132042,6.638208] E3 [2.815359,32.2752]]</p> <p>0.5 order</p> <p>[Normal wear E2 [0.179697,0.864891] E3 [0.778527,8.449168]]</p> <p>[Slight wear E2 [0.161213,0.57485] E3 [1.031164,5.784789]]</p> <p>[Moderate wear E2 [0.134271,0.411952] E3 [1.384597,3.460389]]</p> <p>[Sever wear E2 [0.056887,0.368922] E3 [0.271446,3.539992]]</p> <p>0.7 order</p> <p>[Normal wear E2 [-0.02808,0.004939] E3 [0.078514,0.909913]]</p> <p>[Slight wear E2 [-0.02328,0.007375] E3 [0.102365,0.627765]]</p> <p>[Moderate wear E2 [-0.01261,0.00133] E3 [0.150787,0.370202]]</p> <p>[Sever wear E2 [-0.01093,0.003444] E3 [0.02408,0.381951]]</p> <p>0.9 order</p> <p>[Normal wear E2 [-0.02017,-0.00165] E3 [0.007512,0.095832]]</p> <p>[Slight wear E2 [-0.01372,-0.00249] E3 [0.009548,0.066796]]</p> <p>[Moderate wear E2 [-0.00853,-0.00301] E3 [0.016119,0.038641]]</p> <p>[Sever wear E2 [-0.00831,-0.00075] E3 [0.001804,0.040329]]</p>	<p>0.2 order</p> <p>[Normal wear E2 [9.087177,57.54351] E3 [22.85533,231.9193]]</p> <p>[Slight wear E2 [11.35305,37.50738] E3 [30.72573,157.4507]]</p> <p>[Moderate wear E2 [8.790867,24.83418] E3 [37.53806,95.66855]]</p> <p>[Sever wear E2 [4.174519,24.10283] E3 [8.887816,96.96781]]</p> <p>0.4 order</p> <p>[Normal wear E2 [0.715271,4.011811] E3 [2.41806,25.57791]]</p> <p>[Slight wear E2 [0.807245,2.635989] E3 [3.22144,14.5709]]</p> <p>[Moderate wear E2 [0.616941,1.804728] E3 [4.172277,10.50377]]</p> <p>[Sever wear E2 [0.279937,1.691215] E3 [0.880979,10.70824]]</p> <p>0.6 order</p> <p>[Normal wear E2 [0.020188,0.112158] E3 [0.248523,2.779366]]</p> <p>[Slight wear E2 [0.00743,0.078314] E3 [0.326857,1.909719]]</p> <p>[Moderate wear E2 [0.013289,0.066546] E3 [0.457848,1.134807]]</p> <p>[Sever wear E2 [0.00539,0.05032] E3 [0.081966,1.165508]]</p> <p>0.8 order</p> <p>[Normal wear E2 [-0.03362,-0.00156] E3 [0.024487,0.296248]]</p> <p>[Slight wear E2 [-0.0236,-0.00265] E3 [0.031574,0.205354]]</p> <p>[Moderate wear E2 [-0.0141,-0.00495] E3 [0.049432,0.120034]]</p> <p>[Sever wear E2 [-0.01371,-0.00046] E3 [0.006799,0.1245]]</p> <p>1 order</p> <p>[Normal wear E2 [-0.01003,-0.00097] E3 [0.002255,0.030765]]</p> <p>[Slight wear E2 [-0.00673,-0.00142] E3 [0.00281,0.021584]]</p> <p>[Moderate wear E2 [-0.00426,-0.0015] E3 [0.005224,0.012333]]</p> <p>[Sever wear E2 [-0.00414,-0.00047] E3 [0.000428,0.012968]]</p>
---	---

FIGURE 14. The matter-element models of tool wear for Sprott chaotic systems of different fractional orders.

TABLE 3. Statistics of diagnosis rates for chaotic systems of different fractional orders.

	Lorenz	Chen-Lee	Sprott
0.1order	92.5%	100%	35%
0.2order	100%	92.5%	41.25%
0.3order	100%	95%	33.75%
0.4order	92.5%	100%	38.75%
0.5order	92.5%	100%	38.75%
0.6order	100%	100%	30%
0.7order	100%	93.75%	43.75%
0.8order	96.25%	100%	35%
0.9order	100%	100%	31.25%
1order	100%	92.5%	30%
Average	97.375%	97.375%	35.75%

IV. CONCLUSION

In this paper, three master-slave fractional order chaotic systems, i.e. Lorenz, Chen-Lee and Sprott, are proposed. The boundaries of Centroid of tool wear conditions are located

through the dynamic errors generated using the unique high-sensitivity property of chaotic system. The application of different fractional orders (0.1 to 1) to the system also changes the behavior of dynamic errors, leading to more obvious distribution of characteristics of tool wear conditions. The experiment results demonstrate that, as shown in Figures 8 to 10, intuitive categorization is easier to achieve by using the characteristics of Centroid than the method based on frequency-domain analysis and dynamic errors. The extension distances based on the ranges of Centroid from all fractional order states are used to build matter-element model (as shown in Figures 11 to 13). The current state of cutting tool is then determined by the calculation of relational function. The diagnosis rate is therefore improved by using this method. This study is the first one of the studies of fractional order chaotic theory to compare the dynamic systems based on three different chaotic architectures. Table 2 shows that Sprott system has the lowest diagnosis rate (35.75) of the three. The diagnosis rates of Chen-Lee and Lorenz systems are the same (97.375%) and even reach 100% diagnosis rate at orders 0.6 and 0.9. Both systems exhibit very clear distinction between the distributions of Centroid of cutting tool at order 0.6. Although there exists ambiguity between the moderate and severe wear conditions for Lorenz system at order 0.9, the intelligent categorization achieved with extension theory helps clarify the boundary so that the diagnosis rate can reach as high as 100%. Therefore, Chen-Lee and Lorenz systems of orders 0.6 and 0.9 are chosen to be the architectures for system testing and verification in the future study. This method has the advantages of high accuracy, high reliability and simplicity since it does not need many sensors or long time to extract characteristics. Using this method, users can determine the current condition of the cutting tool and milling accuracy quickly and efficiently.

REFERENCES

- [1] H.-T. Yau, S.-Y. Wu, C.-L. Chen, and Y.-C. Li, "Fractional-order chaotic self-synchronization-based tracking faults diagnosis of ball bearing systems," *IEEE Trans. Ind. Electron.*, vol. 63, no. 6, pp. 3824–3833, Jun. 2016.
- [2] M. Seera, M. L. D. Wong, and A. K. Nandi, "Classification of ball bearing faults using a hybrid intelligent model," *Appl. Soft Comput.*, vol. 57, pp. 427–435, Aug. 2017.
- [3] B. Jinsong, G. Yuan, Z. Xiaohu, Z. Jianguo, and J. Xia, "A data driven model for predicting tool health condition in high speed milling of titanium plates using real-time SCADA," *Procedia CIRP*, vol. 61, pp. 317–322, Mar. 2017.
- [4] Y. Dai and K. Zhu, "A machine vision system for micro-milling tool condition monitoring," *Precis. Eng.*, vol. 52, pp. 183–191, Apr. 2018.
- [5] S. N. Bhagat and S. L. Nalbalwar, "LabVIEW based tool condition monitoring and control for CNC lathe based on parameter analysis," in *Proc. IEEE Int. Conf. Recent Trends Electron., Inf. Commun. Technol. (RTEICT)*, May 2016, pp. 1386–1388.
- [6] F. A. Niaki, D. Ulutan, and L. Mears, "Wavelet based sensor fusion for tool condition monitoring of hard to machine materials," in *Proc. IEEE Int. Conf. Multisensor Fusion Integr. Intell. Syst. (MFI)*, Sep. 2015, pp. 271–276.
- [7] M. A. Elgarni and A. Al-Habaibeh, "Analytical and comparative study of using a CNC machine spindle motor power and infrared technology for the design of a cutting tool condition monitoring system," in *Proc. IEEE 13th Int. Conf. Ind. Inform. (INDIN)*, Jul. 2015, pp. 782–787.
- [8] H.-T. Yau and M. H. Wang, "Chaotic eye-based fault forecasting method for wind power systems," *IET Renew. Power Gener.*, vol. 9, no. 6, pp. 593–599, 2015.

[9] R. Scherer, S. L. Kalla, Y. Tang, and J. Huang, "The Grünwald–Letnikov method for fractional differential equations," *Comput. Math. Appl.*, vol. 62, pp. 902–917, Aug. 2011.

[10] G. Sun, Z. Ma, and J. Yu, "Discrete-time fractional order terminal sliding mode tracking control for linear motor," *IEEE Trans. Ind. Electron.*, vol. 65, no. 4, pp. 3386–3394, Apr. 2018.

[11] Z. Hua, B. Zhou, and Y. Zhou, "Sine-transform-based chaotic system with FPGA implementation," *IEEE Trans. Ind. Electron.*, vol. 65, no. 3, pp. 2557–2566, Mar. 2018.

[12] G. Li and B. Zhang, "A novel weak signal detection method via chaotic synchronization using Chua's circuit," *IEEE Trans. Ind. Electron.*, vol. 64, no. 3, pp. 2255–2265, Mar. 2017.

[13] J.-H. Chen, "Controlling chaos and chaotification in the Chen–Lee system by multiple time delays," *Chaos, Solitons Fractals*, vol. 36, pp. 843–852, May 2008.

[14] C.-H. Huang, C.-H. Lin, and C.-L. Kuo, "Chaos synchronization-based detector for power-quality disturbances classification in a power system," *IEEE Trans. Power Del.*, vol. 26, no. 2, pp. 944–953, Apr. 2011.

[15] L.-J. Sheu, L.-M. Tam, H.-K. Chen, and S.-K. Lao, "Alternative implementation of the chaotic Chen–Lee system," *Chaos, Solitons Fractals*, vol. 41, pp. 1923–1929, Aug. 2009.

[16] H. Wang, K. Sun, and S. He, "Characteristic analysis and DSP realization of fractional-order simplified lorenz system based on adomian decomposition method," *Int. J. Bifurcation Chaos*, vol. 25, no. 6, pp. 1–13, Jun. 2015.

[17] S. Kurada and C. Bradley, "A machine vision system for tool wear assessment," *Tribol. Int.*, vol. 30, no. 4, pp. 295–304, 1997.

[18] C.-B. Fu, A.-H. Tian, Y.-C. Li, and H.-T. Yau, "Fractional order chaos synchronization for real-time intelligent diagnosis of islanding in solar power grid systems," *Energies*, vol. 11, no. 5, p. 1183, 2018.

[19] H.-T. Yau, C.-C. Wang, C.-T. Hsieh, and S.-Y. Wu, "Fractional order Sprott chaos synchronisation-based real-time extension power quality detection method," *IET Gener., Transmiss. Distrib.*, vol. 9, no. 16, pp. 2775–2781, 2015.

[20] H.-T. Yau, Y.-C. Kuo, C.-L. Chen, and Y.-C. Li, "Ball bearing test-rig research and fault diagnosis investigation," *IET Sci., Meas. Technol.*, vol. 10, no. 4, pp. 259–265, 2016.



CHENG-CHI WANG received the B.S., M.A., and Ph. D. degrees in mechanical engineering from National Cheng Kung University, Taiwan, in 1996, 1998, and 2001, respectively. He is currently a Distinguished Professor with the Graduate Institute of Precision Manufacturing, National Chin-Yi University of Technology. He has authored or co-authored more than 150 research articles. He holds 30 patents. His research interests include machine tool, lubrication, nonlinear dynamic analysis and control, and numerical simulations.



JIN-YU CHANG received the B.S. degree in electrical engineering from Kun Shan University, Tainan, Taiwan, in 2016, and the M.S. degree in electrical engineering from the National Chin-Yi University of Technology. His research interests include nonlinear system analysis and control.



HER-TERNG YAU received the B.S. degree from National Chung Hsing University, Taichung, Taiwan, in 1994, and the M.S. and Ph.D. degrees from National Cheng Kung University, Tainan, Taiwan, in 1996 and 2000, respectively, all in mechanical engineering. He is currently a Professor with the Department of Electrical Engineering, National Chin-Yi University of Technology, Taichung. He has authored more than 150 research articles on a wide variety of topics in mechanical and electrical engineering. His research interests include energy converter control, system control of mechatronics, and nonlinear system analysis and control.



XIAO-YI SU received the B.S. degree from the National Chin-Yi University of Technology, Taichung, Taiwan, in 2017, where he is currently pursuing the M.S. degree in electrical engineering. His research interests include nonlinear system analysis and control.

...